# EFFECT OF SINTERING PARAMETERS ON MECHANICAL PROPERTIES OF SINTER HARDENED MATERIALS

**François Chagnon and Yves Trudel**

**Quebec Metal Powders Limited**

ABSTRACT

Sinter hardening is a process where P/M part microstructure transforms partially or completely into a martensitic structure during the cooling phase of the sintering cycle.  The amount of martensite produced and hence the mechanical properties are a function of the hardenability of the alloy,  the mix composition and the cooling rate of the parts.  The latter is affected by the cooling capacity of sintering furnaces,  the size of the parts and the belt loading.  Large parts or heavy belt loading reduces the cooling rate.

The sintering temperature is another variable affecting the mechanical properties of P/M steels.  High temperature sintering increases the densification of P/M parts and modifies  the pore shape thus improving the mechanical properties.  Tests were carried out to evaluate the effect of sintering temperature in a range of 1120 to 1290°C (2050 to 2350°F) on the mechanical properties of specimens made from a low alloy steel specifically designed for sinter hardening applications.  Results are discussed in relation to the microstructure and sintering conditions.

INTRODUCTION

Sinter hardening is becoming a popular process for producing P/M parts with high strength and apparent hardness at lower cost because it eliminates a post sintering heat treatment.  It is well known that quenching P/M parts introduces high thermal stresses and part distortion.  Also,  because of the presence of porosity,  parts must be cleaned before (if containing oil or grease) and after heat treatment [1,2]. Finally,  depending on the size and the amount of porosity,  P/M parts are more difficult to quench than wrought materials.

To obtain optimum microstructures,  prealloyed powders are generally preferred over admixed powders because they allow to minimize the alloying additions for similar strength and hardness [3]. Prealloyed sinter hardening materials enable tighter dimensional tolerances as compared to quenched and tempered parts.  In addition,  with proper material formulation,  sinter hardening can tailor the final microstructure as a function of the size of the parts and the sintering furnace throughput which directly

affect the cooling rate. Design modifications to sintering furnaces now permit higher sintering temperature with better control of cooling rates and allow part producers more flexibility to manufacture P/M part with specific microstructure. The development of prealloyed steel powders specifically designed for sinter hardening applications has also made it possible for part manufacturers to produce large or thin wall parts [4, 5].

The objective of this work was to study the behavior of low alloy steel powders used for sinter hardening applications as a function of the sintering temperature. Test specimens have been characterized for both mechanical properties and microstructure.

EXPERIMENTAL PROCEDURE

The base powder used is this study was ATOMET 4701, a low alloy steel specifically designed for sinter hardening applications. Table 1 shows the typical physical and chemical properties of this powder. After admixing with 2% copper, graphite to reach sintered carbon of respectively 0.65 and 0.80% in the test specimens and 0.75% zinc stearate as lubricant, test specimens were pressed to 6.8 g/cm³. Sintering was performed in industrial furnaces in a 90% nitrogen based atmosphere. The time at temperature was 25 minutes for the tests carried out at 1120°C (2050°F) and 33 minutes for those carried at 1205 and 1290°C (2200 and 2350°F). The cooling rate from 870 to 650°C (1600 to 1200°F) was 0.7°C/s (1.3°F/s) for the specimens sintered at 1120°C. A slightly higher cooling rate, 0.9°C/s or 1.6°F/s was observed on test bars sintered at 1205 and1290°C. All the specimens were tempered one hour in air at 205°C (400°F) before evaluation. Tensile properties were determined using round machined specimens according to MPIF standard 10 while impact energy was measured using Charpy specimens according MPIF standard 40. Dimensional change from die size and apparent hardness were measured on transverse rupture bars. The pore roundness was determined with a Clemex 640 Vision image analyzer. Only pores larger than 7 ?m were considered for this evaluation since very small pores were almost entirely spherical.

TABLE 1
Physical and chemical characteristics of ATOMET 4701.

| Apparent Density g/cm³ | Flow s/50g | C % | O % | S % | Cr % | Mn % | Mo % | Ni % | Fe % |
|---|---|---|---|---|---|---|---|---|---|
| 2.92 | 26 | 0.01 | 0.25 | 0.009 | 0.45 | 0.45 | 1.00 | 0.90 | Bal. |

RESULTS AND DISCUSSION

The measured mechanical properties of ATOMET 4701 specimens containing 2% copper and 0.65 or 0.80% carbon pressed at 6.8 g/cm³, sintered at either 1120, 1205 or 1290°C and tempered for one hour at 205°C are given in Table 2.

Figure 1 illustrates the effect of the sintering temperature on apparent hardness for the two levels of sintered carbon. Apparent hardness increases with the carbon content and sintering temperature. At 0.65% C, the relationship is almost linear while at 0.80% C, apparent hardness increases by 4 HRC from 1120 to 1205°C and remains almost constant from 1205 to 1290°C. Also, the difference in apparent hardness as the carbon content increases from 0.65 to 0.80% is larger at 1120°C than at 1290°C.

These results can be explained by the modification of the microstructure as the carbon concentration and the sintering temperature increase. As shown in Figures 2, 3 and 4, the microstructure is mainly composed of martensite and bainite with few amount of very fine pearlite and retained austenite. Specimens with 0.80% C exhibit larger quantity of lower bainite and martensite than those with 0.65% C. Also, as the sintering temperature increases, the amount of martensite increases. This can be related to

2

the faster cooling rate and also to a better microstructure homogenization reached at 1205 and 1290°C as compared to 1120°C.  Finally,  the amount of retained austenite increases with the carbon content and the sintering temperature.  This may explain why apparent hardness reaches a plateau at 1205°C and 0.80%C.  It is also worth noting that apparent hardness is also dependent on specimen density.  For sintered density of 6.70 to 6.80 g/cm³,  apparent hardness after tempering cannot exceed 32-34 HRC [6] because the microstructure is nearly fully martensitic and cannot overcome the hardness drop caused by porosity.

The effect of sintering temperature on ultimate tensile strength for the two carbon levels is illustrated in Figure 5.  The ultimate tensile strength increases with the sintering temperature.  At 0.65% C,  a gain in UTS of 16.5% is observed as the sintering temperature is raised from 1120 to 1290°C.  It is worth noting that these UTS values ranging from 753 to 877 MPa (109.2 to 127.1 kpsi) achieved with these sintering conditions and a green density of 6.8 g/cm³ compares favourably to those published in the MPIF Standard 35 for heat treated carbon,  copper,  nickel and low allow steels [6].  At 0.80% C,  the sintering temperature has only a minor effect on UTS.  A gain of only 21 MPa or 3% is observed in the range of temperatures studied.  It is worth noting that the UTS is lower at 0.80% C than at 0.65% C.  In a previous study,  it was observed that the maximum UTS for the same sinter hardening material was reached at carbon concentrations ranging from 0.65 to 0.75%[5].  A similar observation was made with heat treated low alloy FL42XX and FL46XX steels which also showed a maximum strength but at carbon contents ranging from 0.40 to 0.50% C [7].  It is assumed that as the sintering temperature rises,  the increase in martensite concentration has shifted the maximum strength value toward lower concentrations of carbon and therefore counterbalanced the beneficial effect of the sintering temperature.

TABLE 2
Properties of tempered specimens as a function of combined carbon and sintering temperature.

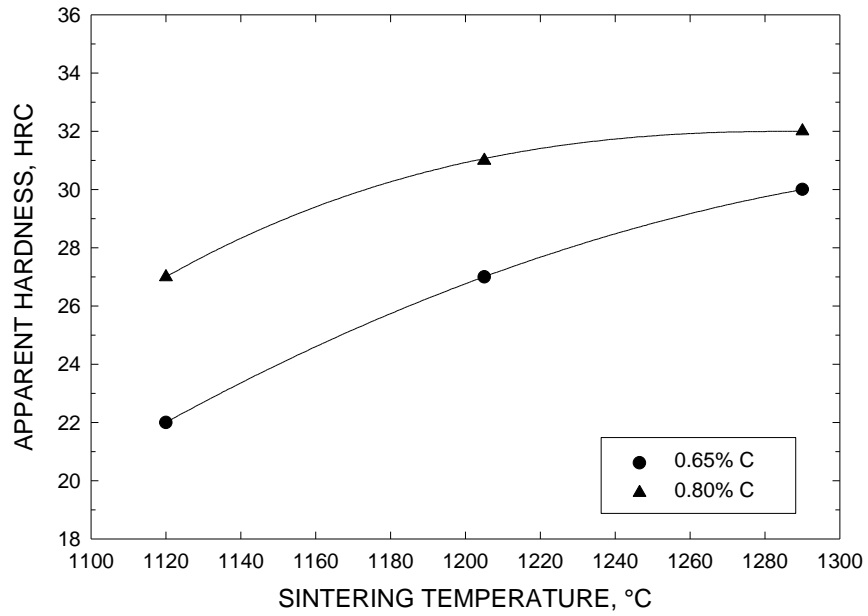| Combined C, % | Sintering Temperature °C | UTS MPa (kpsi) | YS MPa (kpsi) | Apparent Hardness, HRC | Impact Energy J (ft-lb) | Dimensional Change % from die size |
|---|---|---|---|---|---|---|
| 0.65 | 1120 | 753 (109.2) | 649 (94.1) | 22 | 11.3 (8.3) | +0.27 |
| | 1205 | 802 (116.3) | 791 (114.7) | 27 | 11.9 (8.8) | +0.15 |
| | 1290 | 877 (127.1) | 813 (117.9) | 30 | 12.6 (9.3) | +0.09 |
| 0.80 | 1120 | 702 (101.8) | 582 (84.4) | 27 | 10.4 (7.7) | +0.18 |
| | 1205 | 666 (96.5) | 640 (92.8) | 31 | 12.9 (9.5) | +0.05 |
| | 1290 | 723 (104.8) | 693 (100.5) | 32 | 15.6 (11.5) | -0.01 |

Figure 1.  Effect of sintering temperature on apparent hardness of TRS specimens pressed to 6.8 g/cm³, sintered in nitrogen base atmosphere and tempered one hour at 205°C).



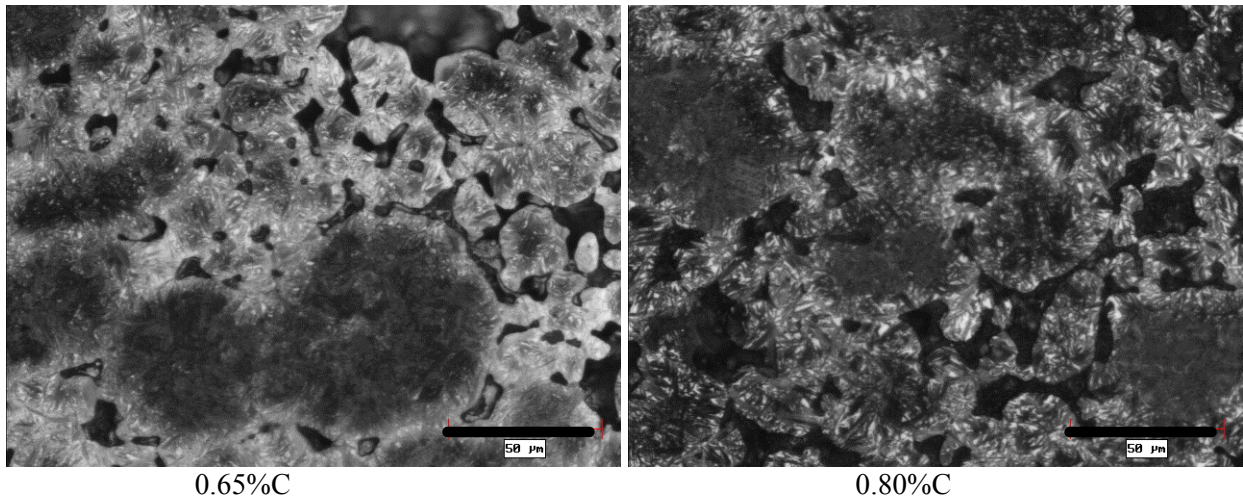0.65%C                                                    0.80%C

Figure 2.  Microstructure of specimens containing 0.65 and 0.80%C sintered at 1120°C.  (Pre-etch with Nital 2% followed by sodium metabisulfite etching).
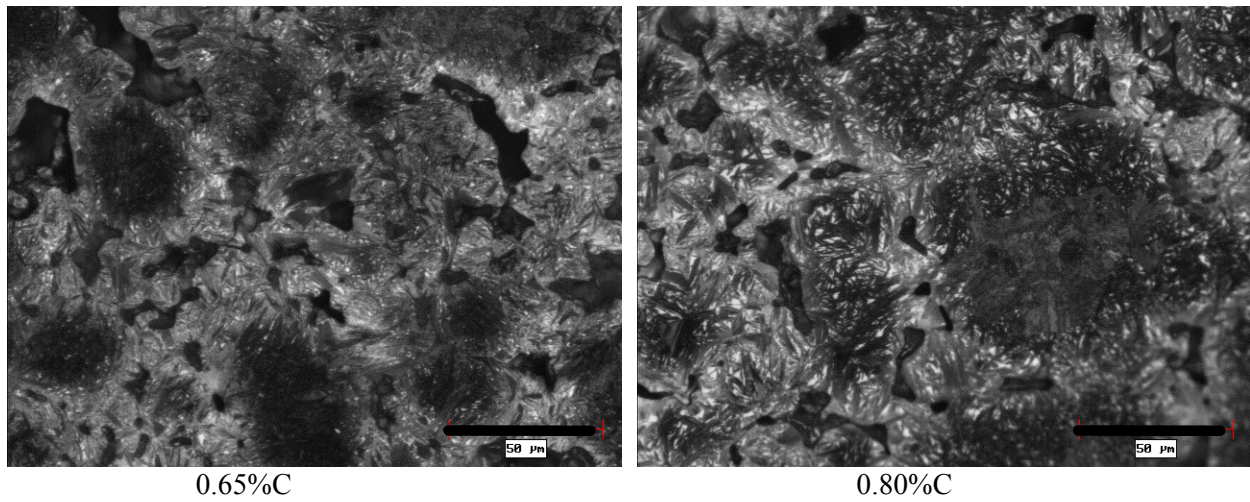
|  0.65%C  |  0.80%C  |

Figure 3  Microstructure of specimens containing 0.65 and 0.80%C sintered at 1205°C.  (Pre-etch with Nital 2% followed by sodium metabisulfite etching).
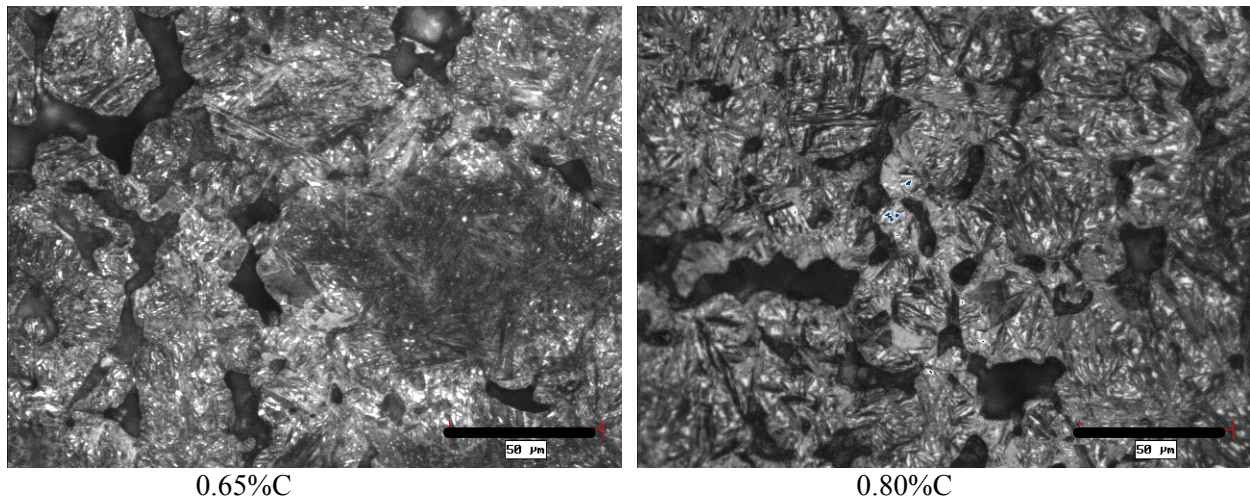



|  0.65%C  |  0.80%C  |

Figure 4.  Microstructure of specimens containing 0.65 and 0.80%C sintered at 1290°C.  (Pre-etch with Nital 2% followed by sodium metabisulfite etching).

Figure 6 shows that the yield strength increases with sintering temperature for both carbon contents but the effect is more pronounced at 0.65%C than at 0.80%C.  The yield strength of the 0.65% C alloy increases by 25% as the sintering temperature is raised from 1120 to 1290°C.  For the 0.80%C alloy this gain is only 19% under the same conditions.  As for the UTS,  the yield strength is lower for the higher carbon content.

The effect of sintering temperature on impact energy is illustrated in Figure 7.  Impact strength increases with the sintering temperature.  This was expected because high temperature sintering favors pore rounding [8].  However the impact of sintering temperature is significantly larger at 0.80%C than at 0.65%C.  A gain of only 12% is observed at 0.65%C as compared to 50% at 0.80%C.  Furthermore,  for the higher sintering temperatures,  the impact energy is greater for the 0.80%C specimens than for those at 0.65%C.  This can be explained by the larger amount of retained austenite and bainite in the higher carbon specimens which could have contributed to improve impact resistance.
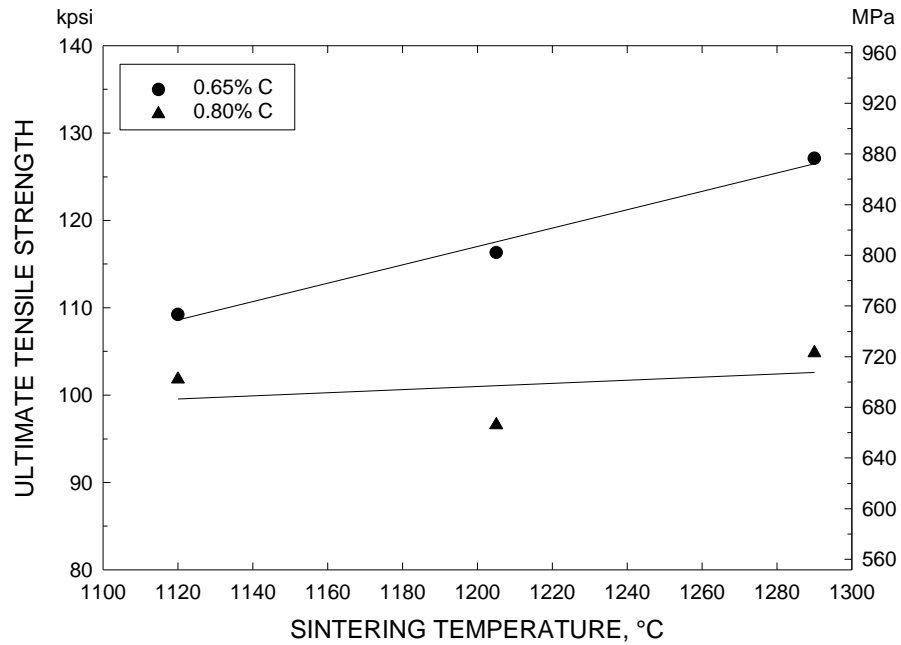
Figure 5.  Effect of sintering temperature on ultimate tensile strength of specimens pressed to 6.8 g/cm³, sintered in nitrogen base atmosphere and tempered one hour at 205°C).
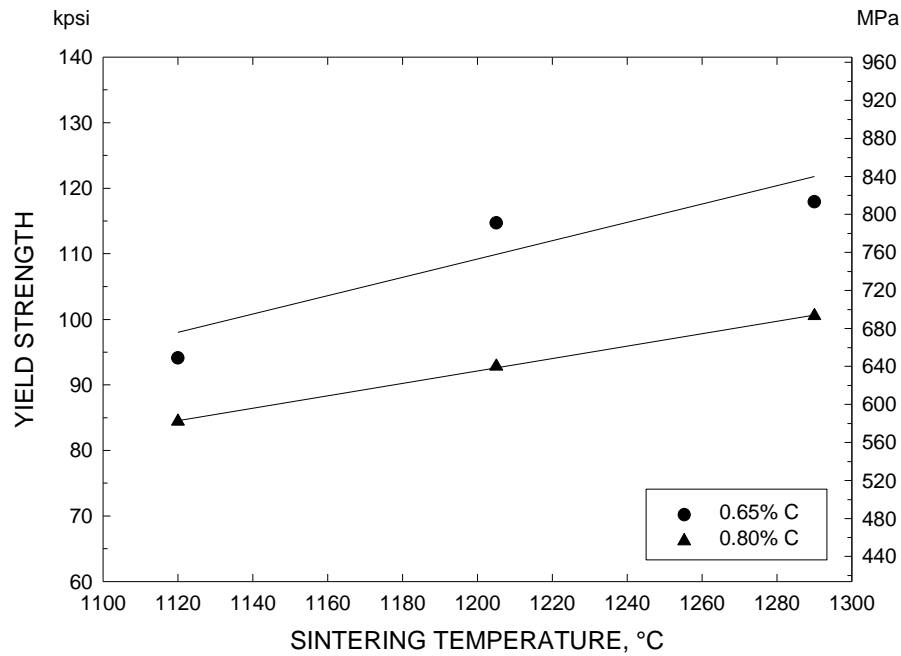


Figure 6.  Effect of sintering temperature on yield strength of specimens pressed to 6.8 g/cm³,  sintered in nitrogen base atmosphere and tempered one hour at 205°C).
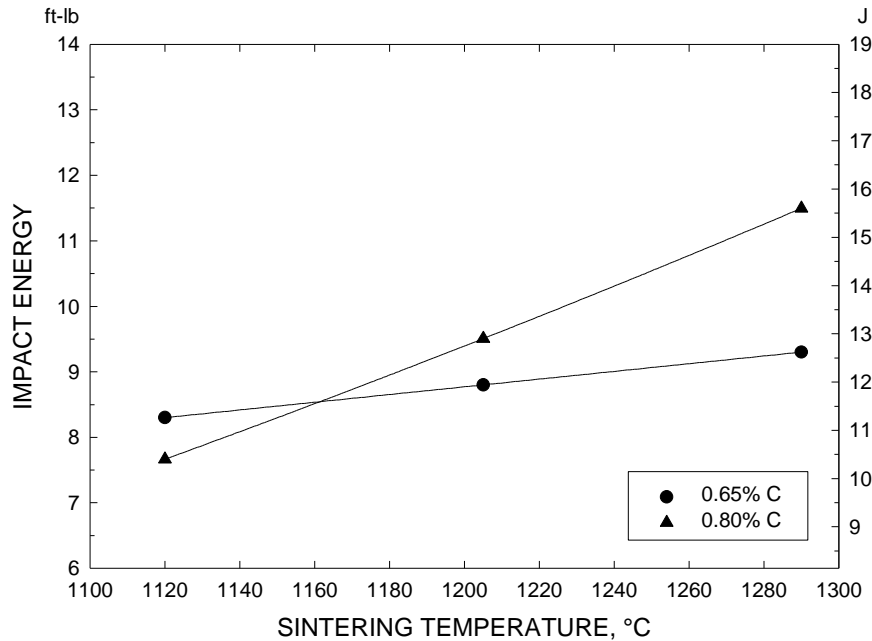
6

Figure 7. Effect of sintering temperature on impact energy of specimens pressed to 6.8 g/cm³, sintered in nitrogen base atmosphere and tempered one hour at 205°C).

Figure 8 illustrates the effect of sintering temperature on dimensional change for the two levels of sintered carbon. One can see similar trends for both carbon levels. The growth is reduced by about 0.18% as the sintering temperature increases from 1120 to 1290°C. Also at 0.80% C, the specimens show less growth than at 0.65% C by about 0.10%. Similar trends are observed with regular P/M copper steels.

Figure 9 illustrates the unetched microstructure of specimens containing 0.8% carbon for the three sintering temperatures. As the sintering temperature increases, the steel particles gradually lose their identity and the pores become more spherical. This behavior is typical of the high temperature sintering process.

Figure 10 illustrates the effect of sintering temperature on the concentration of pores having a shape factor in a range of 0.95 to 1. It is worth noting that a shape factor of one corresponds to a perfect sphere. Also, only pores larger than 7 ?m were considered for this part of the study, small pores being almost entirely spherical. As expected, the proportion of spherical pores increases with the sintering temperature. Also, the 0.80% C specimens show a larger proportion of spherical pores than those containing 0.65% C. Presumably, the small graphite particles diffuse into the steel matrix, they leave small pores which easily become round at these sintering temperatures.
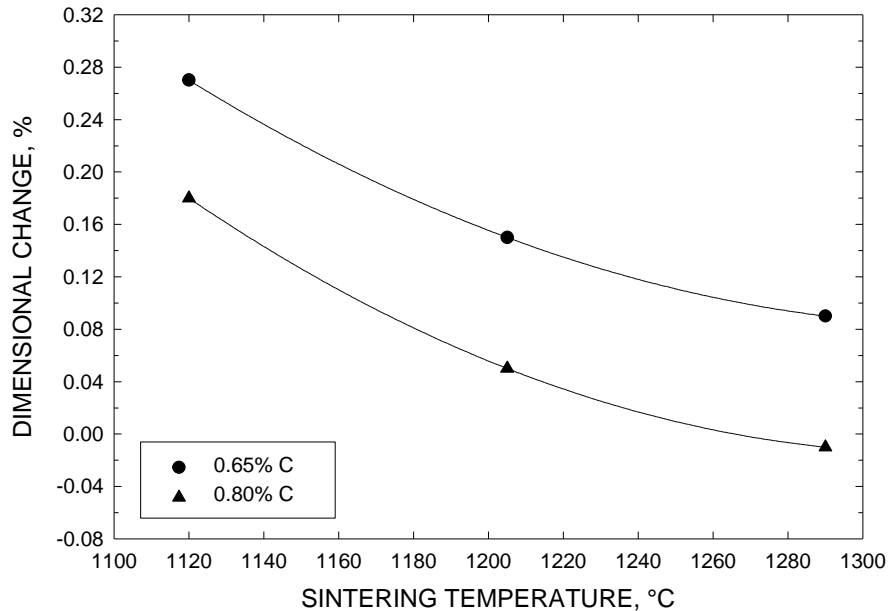
Figure 8. Effect of sintering temperature on dimensional change from die size of TRS bars pressed to 6.8 g/cm³, sintered in nitrogen base atmosphere and tempered one hour at 205°C).

CONCLUSIONS

1. Apparent hardness increased with sintering temperature and carbon content. An apparent hardness of 32 HRC was reached with specimens containing 0.8% C and 2% Cu after sintering at 1290°C and tempering one hour at 205°C. The sintering temperature had a more pronounced effect on the 0.65%C specimens as compared to those containing 0.80% C.

2. Specimens containing 0.65% C exhibited a higher UTS than those containing 0.8% C. Also, specimens containing 0.8% C were less affected by the sintering temperature than those containing 0.65% C. UTS of 880 MPa (128 kpsi) was reached at 1290°C and 0.65% C for specimens pressed to 6.8 g/cm³.

3. Impact energy increased with the sintering temperature but the effect was more pronounced for the 0.8% C specimens. This was caused by a greater amount of retained austenite and bainite present in these specimens as compared to those containing 0.65%C.

4. Growth decreased by about 0.18% when increasing the sintering temperature from 1120 to 1290°C and by about 0.10% when the carbon content was increased from 0.65 to 0.8%.

5. The proportion of spherical pores increased with the sintering temperature and the carbon content, the latter being probably related to the larger amount of voids left by the diffusion of the graphite particles into the steel matrix.
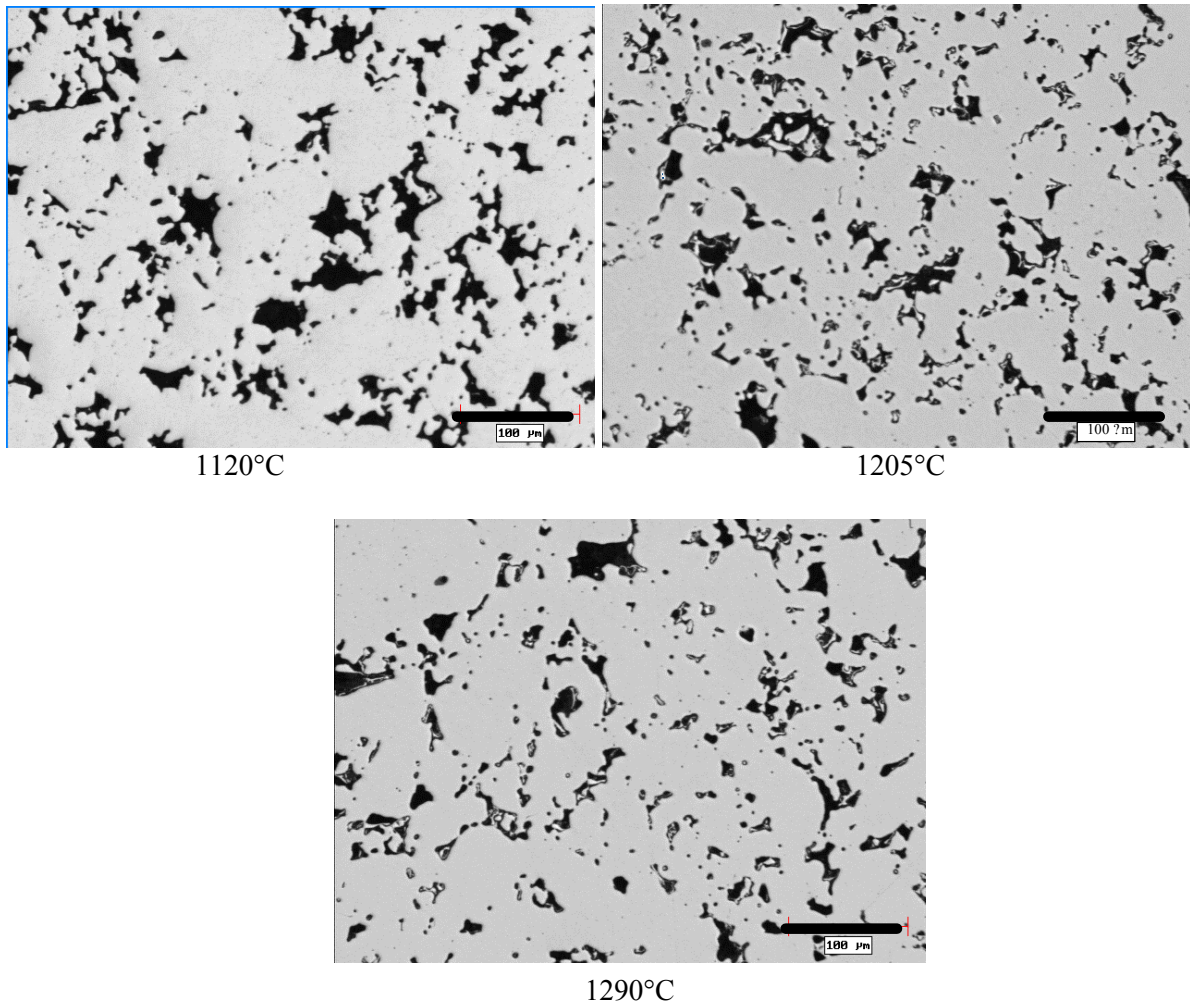
1120°C



1205°C



1290°C

Figure 9.  Specimen microstructure (as polished) for the various sintering temperatures.
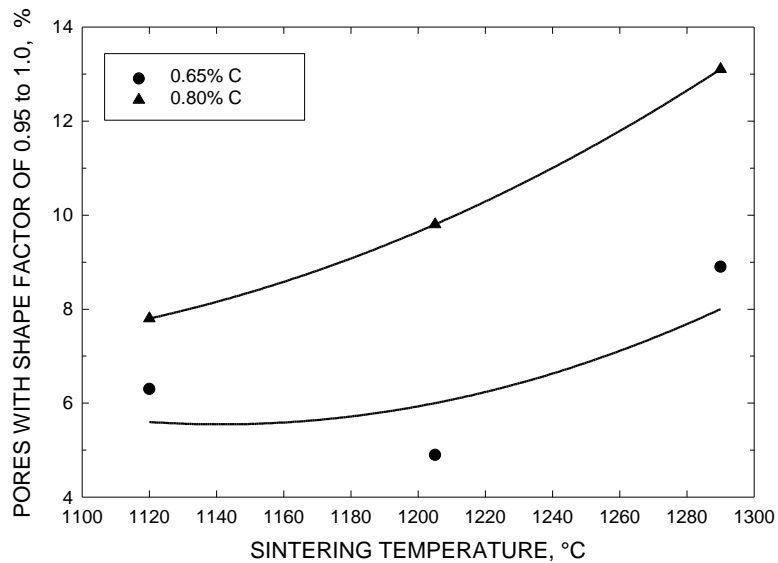


Figure 10  Effect of sintering temperature and carbon content on proportion of pores with a shape factor in the range of 0.95 to 1.

REFERENCES

1. R. Ratzi, "Modern Methods for the Heat Treatment of High Strength Sintered Parts", In-House PM Seminar on Advanced PM Components for the Automotive Industry, Adam Opel AG, EPMA, June 21, 1993.

2. H. Ferguson, "The Heat Treatment of P/M Steels-an Overview", Proceedings of the 16th ASM Heat Treating Society Conference & Exposition, 19-21 March 1996, Cincinnati, OH.

3. R. Ratzi and P. Orth, "Microstructure and Properties of Ferrous P/M Products", Paper presented at the 1996 Deformation and Fracture in Structural PM-Materials, 13-16 October 1996, The High Tatras, Slovakia.

4. F. Chagnon and Y. Trudel, "Designing Low Alloy Steel Powders for Sinterhardening Applications", Advances in Powder Metallurgy & Particulate Materials-1996, MPIF, Princeton, N.J., 1996, p.13-211.

5. C. Ruas and F. Chagnon, "The Development and Characteristics of Low Alloy Steel powders for Sinterhardening Applications", Paper presented at the PM97 International Conference on Powder Metallurgy for Automotive Components in New Delhi, February 10-12, 1997, PMAI.

6. MPIF Standard 35, Materials Standards for P/M Structural Parts; published by Metal Powder Industries Federation; Princeton. N.J., 1994.

7. H.I. Sanderow and T. Prucher, "Mechanical Properties of Low Allow Steels: Effect of Composition, Density and Heat Treatment", Advances in Powder Metallurgy & Particulate Materials-1994, Vol. 7, MPIF, Princeton, N.J., 1994, p.355-366.

8. S. Mocarski and D.W. Hall, "High Temperature Sintering of Ferrous Powder Metal in Nitrogen Base Atmosphere", New Perspectives in Powder Metallurgy, Vol. 9, MPIF, Princeton, N.J., 1990, p.191.